Threshold ionization energy of an ammoniated chlorine anion proximate to a metal surface

D. M. Hollox
Department of Physics, University of Texas at Austin, Austin, Texas 78712
(Received 11 March 1991; revised manuscript received 18 June 1991)

The excess electronic binding energy of an ammoniated chlorine anion is evaluated using an iterative pseudospectral method of solution. By using a continuum model for the solvent, the potential well is represented in terms of a self-consistently evaluated, induced polarization potential added to a known electron-affinity term. The oxidation-reduction pair energy difference and threshold ionization energy of the complex are calculated with results that are shown to be consistent with experimental values. The effect of a nearby flat metal surface on the excess electronic state is examined and it is shown that the binding energy increases and the oxidation-reduction pair energy difference decreases as the anion approaches the interface.

INTRODUCTION

Localized electron states produced by the solvation of excess negative charges present in polar fluids have been a matter of extensive interest for several decades. The solvated electron, being a self-trapped excess electronic charge confined by an induced alignment of surrounding polar molecules, has received the widest attention but remains an incompletely understood system. The earliest consideration of the ammoniated electron by Jortner[1,2] used this self-induced or Landau potential and assumed that the polar liquid admitted a spherical cavity of at least 3 Å in radius in which the excess electron centrally resided but where appreciable charge density protruded well into the medium. The solvent was assumed to be a continuum characterized by optical and static dielectric constants which entered into the definition of the induced polarization potential occurring outside the cavity, with the interior being modeled with a pseudopotential. While such a model produced reasonable results it did not consider a number of additional factors that would likely modify the solvated state, such as the discrete nature of the oriented polar molecules, the conduction band energy of the initial quasifree electron, or the energy expended by the system through the forced rearrangement of the polar molecules. Semicontinuum models in which the molecular dipoles are considered discrete throughout the first coordination layer before yielding to a continuum have been investigated by several groups such as Copeland, Kestner, and Jortner[3] and Webster and Carmichael.[4] Such models present a more realistic picture of the solvated electronic state as well as eliminating the need to rely on an arbitrary pseudopotential representation within the potential well center. Unfortunately the increasing sophistication of the charge-solvent interaction model has not yet led to substantial improvement in our ability to predict solvation energies for excess electrons in polar liquids.[4] While the solvated electron remains an open problem, there are other excess-electron calculations where a continuum model alone for the ambient medium produces results that are known to be consistent with experimental findings. For example, Stampfli and Benneman[5] have used a continuum model to substantiate the observed electron affinity of larger clusters of ammonia molecules. Similarly a quantum path-integral molecular-dynamics method has been used to demonstrate tight binding of excess electrons to water clusters with a coordination number of at least 8.[6] For water, it has been shown that even a dimer will weakly bind an excess electron through electron-induced dipole interactions with the water molecules.[7]

Solvated excess charges in polar fluids may also be in the form of solvated ions such as Li^+ or Br^-. The theoretical consideration of the solvated ion problem has been more narrowly centered about the evaluation of solvation energies or the free-energy change per mole of gaseous ions introduced into a liquid and allowed to form solvated states. The energetics involved with anionic solvation are equally complex as those of the solvated electron except that the potential well in which the anionic excess electron is localized includes the vacuum electron affinity of the neutral species. An additional complication associated with the continuum model for the solvent in a solvated ion problem is that the dielectric behavior of the medium may not be constant, but often will adopt a value close to the optical dielectric constant in the immediate vicinity of the ion before increasing toward the bulk value at greater distance from the ion. This may occur because the first solvation layer contracts toward smaller ions[8] such as Li^+ or F^-, resulting in the partial immobilization of these molecules, which in turn can restrict the movements of second coordination layer molecules. The immobilized dipoles will then produce an additional contribution to the potential which may be handled through the introduction of a discrete charge distribution.[9] The local dielectric behavior is considered by dividing the solvation sphere into multiple shells each characterized by its own dielectric constant before eventually yielding to the bulk value at a sufficiently large distance from the ion[10–12] However, larger monovalent ions do not produce significant contraction of the first solvation layer, so the physical behavior of the surrounding solvent molecules is not markedly different from that of the bulk molecules. Alternatively one can ascertain whether or not a

discretization of the ion-solvent molecular interaction leads to improved results for the solvated ion problem, such as by modeling the solvent environment by a field of dipoles.[13–15] Another tested method is the molecular-orbital technique, which models the ionic environment with predetermined fractional charges located at the surrounding atomic centers.[16]

In this paper we will consider the case of an excess anion present in a polar liquid which may be bounded by a conducting surface. Instead of calculating the solvation energy of the ion we will directly evaluate the ionization energy of the excess bound electron with respect to the photoelectric threshold using a known vacuum electron-affinity term in the Hamiltonian. The calculation also considers the effect of induced positive image charge density within a nearby flat metal surface on the configuration energy of the excess electron as a function of ion-interface distance.

As noted above the solvated ion problem is similar to the solvated electron case in the sense that both versions of the excess charges are self-trapped by the induced orientation of surrounding polar molecules. The anionic excess electron, however, differs from the single-electronic state in that the excess charge is already residing in the electron-affinity potential well of an ion having a finite core radius. This removes the necessity of creating a void within the fluid in order to produce a localized electronic state, as well as construction of a cavity-size-dependent pseudopotential before invoking a continuum model for the solvent. For most atomic anions the hard-core radius is known and the preexisting potential well in which the excess electron is trapped can be described accurately.[17] Thus the main problem in evaluating the excess electronic binding energy of a solvated anion lies in describing the behavior of the Landau potential and its contribution to the overall configuration energy of the stable state. Since the excess electronic charge density will not be a known function, the evaluation of the wave-function-dependent Hamiltonian for the self-trapping model will be performed self-consistently starting from a suitable trial wave function.

AN ISOLATED SOLVATED ANION

As a specific case, we consider the excess electronic binding energy of a Cl^- ion present in liquid ammonia, which has a total bulk dielectric constant of 24.2 at 233 K. A continuum model characterized by a bulk dielectric constant will be used for the solvent since it is known that local dielectric behavior is relatively unimportant for the larger halide ions.[18] The calculation is performed using a discrete iterative spectral method of solution[19] employing a uniformly discretized rectangular coordinate system centered at the chlorine nucleus. This method is attractive computationally because of the relative ease with which the kinematic term is evaluated by using a fast Fourier transform on an initial trial wave function ψ_0 followed by multiplication by the local value of k^2 on the conjugate momentum space grid. An inverse fast Fourier transform is then performed on this new array, which is then added to $V\psi_0$ to obtain $H\psi_0$, where V is a potential defined on the original configuration space grid. Furthermore, this method lends itself to a direct iterative eigenvalue method,[20,21] called the shift-power method, which accelerates convergence to the ground eigenstate. This is achieved by normalizing $H\psi_0$, which is defined to be ψ_1, which is the new vector used in the subsequent iteration. Repeating this process often enough will allow the shift-power method to align the wave function along the ground-state eigenfunction of the Hamiltonian thereby yielding the ground-state eigenvalue. The calculation is done in rectangular coordinates since the induced part of the potential is done self-consistently by using Cartesian tensor product cubic spline functions[22,23] to model wave-function-dependent terms in the Hamiltonian. Since the integrands are factorized, integrations over charge-density-dependent terms reduce to a sequence of one-dimensional integrals which may easily be evaluated in order to obtain the induced potential well function. Adding this expression to the vacuum electron-affinity term and the kinematic term produces the complete trial Hamiltonian. The self-consistent aspect of this method of solution is implemented by multiplying the induced potential well associated with the nth iteration by 0.85, which is then added to 0.15 times the nth$+1$ evaluation of the induced potential well to arrive at the nth$+1$ induced potential well function. With this method we can attain convergence to the ground state in 20 iterations or less so that an extravagant use of computer resource time is not required. Atomic units are initially used for convenience with a grid spacing of $0.4a_0$ on axes extending outward from the nucleus $10a_0$ in each direction. The hard core radius of the Cl^- ion[24] is 1.81 Å or $3.4a_0$. Assuming that there is no significant depression of the bulk dielectric constant in the first solvation layer, one must still allow for a smooth transition from the polarized external medium designated by a bulk dielectric constant, to the screened inaccessible interior of the ion where the dielectric constant is usually taken to be 1.[10,12] This is achieved by defining a sharp, continuous, monotonic inward reduction of the value of the dielectric constant near the hard-core radius of the ion. In this calculation a spherical shell of thickness a_0 centered at a distance of $3.3a_0$ from the ionic nucleus is defined within which the dielectric constant is smoothly lowered to 1. Within $2.8a_0$ of the nucleus the self-trapping potential is assumed to be inactive, whereas beyond a distance of $3.8a_0$ the Landau potential acts with full effect on the excess electronic wave function. The section of the grid where $\epsilon=1$ does not imply extreme dielectric saturation since it lies entirely internal to the ion comprising only the core 2.2% of the total grid volume. The shell is centered $0.1a_0$ inside the hard-core ionic radius in order that the number of transition shell grid points falling within the ion is more equal to the number of these grid points lying outside the ionic radius. This allows the screened ionic interior and the fully polarized external environment to equally contribute to the transition in dielectric behavior from the medium into the ion. Within the transition shell each grid point carries a factor $[(r-2.8)/\Delta r]^{l+1}$, multiplying the induced potential, where r is the associated nuclear distance, Δr is the shell thickness, and l is the order

of the multipole term contributing to the polarization potential given in Eq. (6). Thus the Coulombic terms will vanish linearly, the dipole terms quadratically, and so on for the higher-order terms through the transition shell. In this case $\Delta r = a_0$, which is almost as short a distance as possible that a smooth transition can be represented on this grid.

If r is the radial distance from the Cl^- nucleus it has been shown[25] that the potential well which binds the excess electron within the ion takes the form

$$\Phi_I(r) = \frac{-2Z}{r}\Omega(r) , \tag{1}$$

where

$$\Omega(r) = [\mathcal{H}(e^{r/d}-1)+1]^{-1} \tag{2}$$

with the parameters $\mathcal{H}$ and d taken as 3.724 71 and 1.2065, respectively, for the $Z=17$, Cl^- ion. Since this term appears in the radial Schrödinger equation it must be readjusted to our Cartesian equation which has no centrifugal repulsive term. This can be done by removing the factor r from the denominator and multiplying by an additional variational parameter α, chosen so as to yield the known electron affinity of 0.2659 Ry. In this case we have found that, if $\alpha = 0.6094$, the adjusted potential well yields the correct excess electronic binding energy for the chloride ion.

Suppose $\Phi_e(\mathbf{x})$ is the electrostatic potential produced by the excess electronic charge density $\rho(\mathbf{x})$ in an ion nucleus centered coordinate system. Then, if the polar medium is characterized by the bulk dielectric constant ϵ, the induced reaction potential is

$$\left[\frac{\Phi_e(\mathbf{x})}{\epsilon} - \Phi_e(\mathbf{x})\right] = \Phi_p(\mathbf{x}) \tag{3}$$

and the interaction of the excess charge with this potential is

$$e\Phi_p(\mathbf{x}) = -(1-\epsilon^{-1})e\Phi_e(\mathbf{x}) . \tag{4}$$

Thus

$$e\Phi_p(\mathbf{x}) = -(1-\epsilon^{-1})e\int \frac{\rho(\mathbf{x}')}{|\mathbf{x}-\mathbf{x}'|} = -2(0.955\,36)\int \frac{|\psi(\mathbf{x}')|^2}{|\mathbf{x}-\mathbf{x}'|}d^3x' , \tag{5}$$

where the factor 2 appears and the factor e^2 vanishes on adopting atomic units with the integral being evaluated over all space. Since there is only one vacant $3p$ orbital remaining before the anion adopts a closed-shell configuration, we can assume without loss of generality that the excess electron occupies a $3p_0$ state and the inverse distance relation reduces to

$$\frac{1}{|\mathbf{x}-\mathbf{x}'|} = \sum_{l=0}^{\infty}\frac{r_<^l}{r_>^{l+1}}P_l(\cos\theta')P_l(\cos\theta) \tag{6}$$

in spherical coordinates for a system possessing azimuthal symmetry. Thus if $r_< = r'$ and $r_> = r$, the polarization potential becomes, in Cartesian coordinates,

$$\begin{aligned} e\Phi_p(x,y,z) = -(1.910\,71)\int_0^z\int_0^y\int_0^x |\psi(x',y',z')|^2 \Bigg[& \frac{1}{(x^2+y^2+z^2)^{1/2}} + z'\left[\frac{z}{(x^2+y^2+z^2)^{3/2}}\right] \\ & + [\tfrac{3}{2}z'^2 - \tfrac{1}{2}(x'^2+y'^2+z'^2)]\left[\frac{3}{2}\frac{z^2}{r^5} - \frac{1}{2r^3}\right] \\ & + [\tfrac{5}{2}z'^3 - \tfrac{3}{2}z'(x'^2+y'^2+z'^2)]\left[\frac{5z^3}{2r^7} - \frac{3z}{2r^5}\right] + \cdots \Bigg] dx'\,dy'\,dz' \end{aligned} \tag{7}$$

where $(x^2+y^2+z^2)^{1/2}$ is replaced by r for convenience in the higher-order terms. Interchanging the primed and unprimed variables within the large square brackets, the ellipsis in Eq. (6) gives the polarization potential for the case $r_> = r'$ and $r_< = r$. Adding this expression to Eq. (7) gives us the complete induced polarization potential. In this calculation all contributions through $l=5$ were included in the polarization potential. Each integrand is expressed as a three-dimensional B-spline function in the factorized form,

$$f(x,y,z) = \sum_{l=1}^{n}\sum_{j=1}^{n}\sum_{i=1}^{n} c_{ijk}r_i(x_i)s_j(y_j)t_k(z_k) , \tag{8}$$

where r, s, and t are cubic Hermite basis splines associated with each grid point along the x, y, and z axes, respectively. After retaining the spline coefficients c_{ijk}, used to model the presented samples of a particular integrand, the basis splines are then integrated one at a time to obtain a representation of the integral function. In order to maintain a consistent normalization scheme each term appearing in the complete induced polarization potential expression is evaluated separately before summing to obtain the polarization potential function. As noted above Φ_p vanishes within the core ion and is smoothly activated through a surrounding thin transition shell before allowing its full effect in order to facilitate the smooth onset of polarization effects as well as maintaining numerical stability.

Starting from the initial trial wave function $\psi_0 = ze^{-r/1.3}$ (normalized by our iterative procedure) for the excess electron in an isolated Cl^- ion, convergence to the ground-state configuration energy is attained after 17 iterations with a result of 0.615 Ry ±0.002 Ry or 8.4 eV. It has been observed[26,27] that the threshold ionization energy of a hydrated Cl^- ion is 8.8 eV. Substituting the

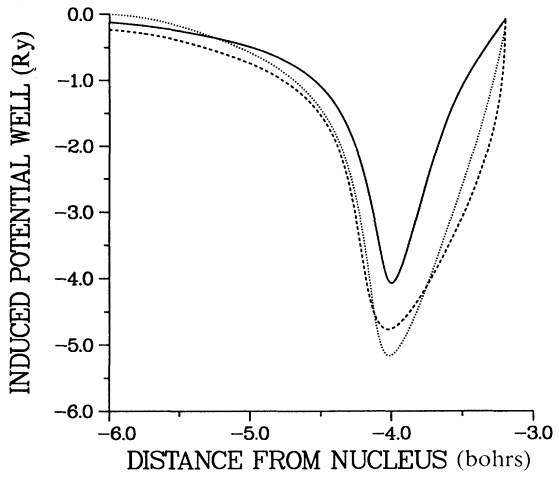

FIG. 1. Induced potential wells, in the polar fluid (ammonia) along the axis normal to the metal surface and passing through the ion nucleus. The dotted curve is associated with a nucleus-interface distance of $6.0a_0$ (bohrs) and the dashed curve represents the $10.0a_0$ example. The solid curve is the induced polarization reaction potential well for the isolated anion. Energies are in units of rydbergs.

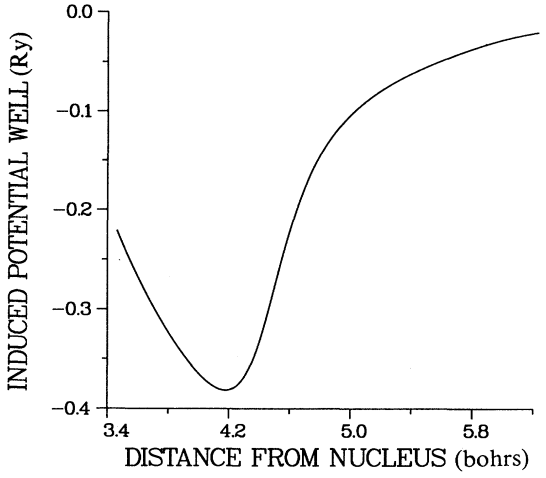

FIG. 3. Induced polarization reaction potential well for the isolated anion along the diagonal line which forms a 45° angle with respect to both the longitudinal (z) axis and the $z=0$ plane in an ion nucleus centered coordinate system.

dielectric constant for ammonia in the factor $(1-\epsilon^{-1})$ would depress this ionization energy by about 0.2 eV, leaving our theoretical value of 8.4 eV about 2.5% less than the anticipated experimental result. In Figs. 1 and 2 the solid curves are the induced reaction potential wells along the longitudinal ($m=0$) axis. As one might expect, a deep valley occurs immediately outside the defined transition shell limit of $3.8a_0$. Notice that the induced reaction potential well is essentially confined within a distance of several a_0. In Fig. 3 a graph of the induced potential well along a diagonal line forming an angle of 45° with respect to each of the positive x, y, and z axes is shown. Notice that the energy scale is about a factor of 10 finer than that of Fig. 1, illustrating the pronounced angular dependence of the induced reaction potential associated with an independently considered $3p$ state. This potential is not equivalent to the potential associated with the orienting field experienced by the actual finite dipoles. The oriented dipoles allow one to define a reactive continuum on which the excess electronic charge density is defined, allowing one to self-consistently evaluate a reaction potential which must possess the same symmetry as the excess electronic charge density. The relative

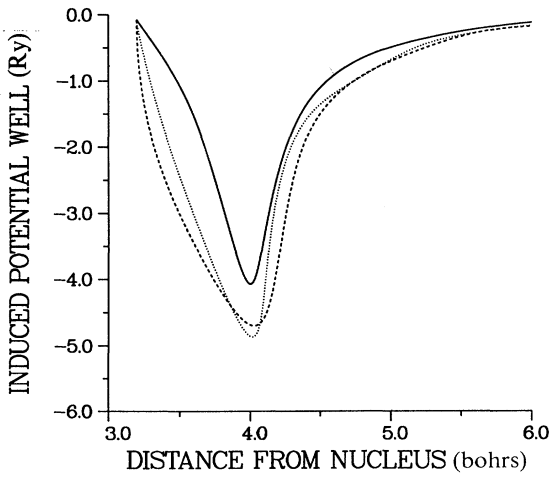

FIG. 2. Induced potential wells along the same axis as that of Fig. 1, but on the opposite side of the ion nucleus (i.e., away from the metal surface). Curve types conform to those of Fig. 1.

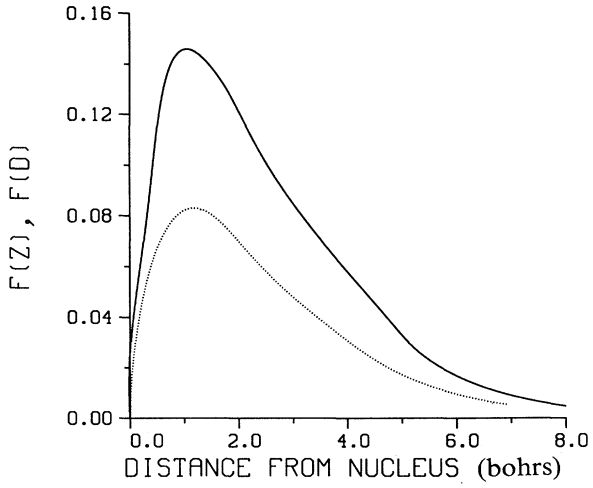

FIG. 4. Wave-function profiles for the excess electron along the longitudinal axis (z) and diagonal line (D) of Fig. 3. Both wave functions are normalized.

strength of the reaction potential along the longitudinal axis is a reflection of this symmetry as well as of the significance of the higher-order terms in the induced potential expression. One may imagine this potential well as having the shape of a trough with its nadir line along the longitudinal axis while steeply rising to essentially zero in the plane-perpendicular to the z axis. In Fig. 4 the corresponding excess electronic wave-function profiles are presented. Notice that the wave-function amplitudes peak well inside the ionic radius before dropping to a relatively small value at a distance of $6a_0$ from the nucleus. Unlike the solvated electron the solvated anionic electron is mainly confined within the first coordination layer of solvent molecules.

ANION IN PRESENCE OF METAL SURFACE

Suppose the anion is allowed to approach a flat metal surface. Due to the electron-electron image interaction, the Hamiltonian acquires the additional term

$$V_{\mathrm{IM}} = -2/\epsilon_\infty z \ , \tag{9}$$

in atomic units, where ϵ_∞ is the optical dielectric constant of liquid ammonia and $z > 0$ is the distance normal to the interface. It is the optical dielectric constant which attenuates the interaction since the intervening medium cannot react to the fast movement of the electron-electron image pair. For liquid ammonia $\epsilon_\infty = n^2 = 1.756$. The presence of positive image charge density has an additional effect beyond that of the electron-electron image attraction. Since the image charge is positive, the associated image potential weakens the induced polarization field associated with the excess negative charge, so that the polarization term weakens as the anion approaches the interface. Thus an additional competing series of terms similar to those involved in the isolated ion induced potential must be added to our previous induced polarization potential expression to form an image charge modified polarization potential. Notice that the magnitude of the electron image charge density is just the real excess electron charge density rotated through 180° about an axis along the metal interface. If the origin of the coordinate system is relocated to the interface at the point collinear with the longitudinal axis through the ionic nucleus, then the distance r' from the origin to a real charge element will equal the distance r'' to the accompanying image charge element, Thus by azimuthal symmetry the image charge element forms an angle $\pi - \theta$ with respect to the axis normal to the interface if the real charge element forms angle θ. Since $\cos(\pi - \theta) = -\cos(\theta)$, the addition of the image terms to the reaction potential results in the vanishing of all l = even terms and a multiplication by 2 of all l = odd terms. An additional factor of 2 is acquired by integration over the image grid. Thus the complete induced potential well is the sum of the electron-electron image interaction with the modified induced polarization expression.

We take the Cl^- nucleus to be located at distances of $6.0a_0$ and $10.0a_0$ from the metal surface. The dotted lines in Figs. 1 and 2 represent the induced potential wells for the $6.0a_0$ case toward and away from the metal surface along the longitudinal axis, respectively, and the dashed lines correspond to the $10.0a_0$ case. The electron-electron image term is cut off at a distance of a_0 from the surface as it is necessary to allow the wave function to vanish at a distance of the order of an atomic radius from the first layer of metal nuclei. Notice that the induced potential well is broadened and does not rise as sharply to the left as does the isolated ion reaction potential. This is due to the increasing strength of the electron-electron image attraction in the immediate vicinity of the metal surface. Also notice that the potential well minimum is about 1 Ry deeper for the $6.0a_0$ ion than for the isolated ion indicating the presence of an attractive interaction with the metal surface. Notice in Fig. 2 that the outer potential well minimum is almost as deep as the potential well toward the surface even though the further potential well minimum is about 5 times farther away from the metal surface. This occurs because the electron-electron image term as well as the competing positive image charge-density contribution to the potential well both weaken with increasing distance from the metal surface. Since these two effects are complementary, the overall contribution of both of these terms to the potential well curve is less than the size of the contribution of either one alone. In Fig. 5 the wave function profile along the longitudinal axis is shown for the $6.0a_0$ example. The two lobes are most distinctive away from the nucleus where the inner lobe vanishes at a distance of $6.0a_0$ due to the presence of the surface but the outer lobe still has about $\frac{1}{8}$ of the maximum wave-function amplitude at the same distance. Notice that the outer lobe profile has a conspicuous "tail," which has a perceptible amplitude at a distance of $10.0a_0$ from the nucleus. Both lobe profiles peak at a distance of about $1.2a_0$ from the

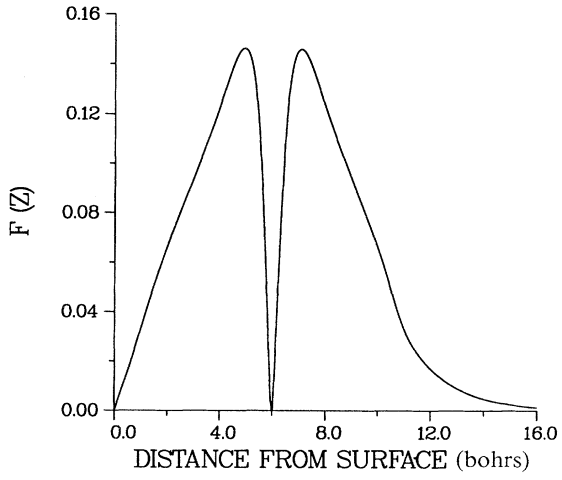

FIG. 5. Wave-function profile for the excess electron along the longitudinal axis when the ion nucleus is positioned $6.0a_0$ from the metal surface.

nucleus, but the inner lobe vanishes almost linearly with decreasing distance to the surface.

Returning to Figs. 1 and 2 we observe that the potential well minima for the $10.0a_0$ example are not as deep as those for the $6.0a_0$ case, although the difference for the outer well is not large. Also observe that the $10.0a_0$ curve is broader than the $6.0a_0$ curve, except near the potential well minima. Both curves are broader than the isolated ion curve because of the gradients in the electron-electron image and image charge induced polarization potentials which are nonexistent in the isolated ion case. The $6.0a_0$ curve is sharper due to the compression of the associated wave function by the metal surface as well as the cutoff in the electron-electron image term near the interface. The outer potential well for the $10a_0$ case more nearly imitates the behavior of the inner potential well because of the weaker gradients in the surface related potentials at this distance from the interface.

The curve in Fig. 6 represents the excess electronic configuration energy as a function of distance from the surface. The curve bends sharply downward as the anion near the surface yielding a binding energy of 0.69 Ry or 9.4 eV at a Cl^- nucleus distance of $6.0a_0$ from the metal, which is about 11% deeper than the isolated ion value. Thus the vertical ionization energy of a solvated anionic electron increases as the anion approaches a metal surface. The increasing configuration energy of the excess electron with decreasing distance to the metal surface shows that the electron-electron image attraction is more significant to the complete binding energy than the competing image charge contribution to the induced potential. This is because the electron-electron image contribution increases more rapidly with decreasing ion nucleus distance to the surface than does the decreasing medium polarization contribution. Also notice that the curve in Fig. 6 becomes relatively flat with increasing distance from the interface, meaning that the excess electron remains more highly bound than the isolated anionic electron at substantial distance into the medium. Even at a distance of $20a_0$ the binding energy is still about 2% greater than for the isolated ion example. This is due to the substantial inability of the medium to screen the electron-electron image pair from each other along their instantaneous vector. The shape of the curve appearing in Fig. 6 suggests that a distance of $50a_0$ or more from the metal surface may be needed in order for one to consider an ion to be isolated. The nucleus is not brought within $6.0a_0$ of the surface because the integrity of the intervening medium becomes questionable at such short distances.

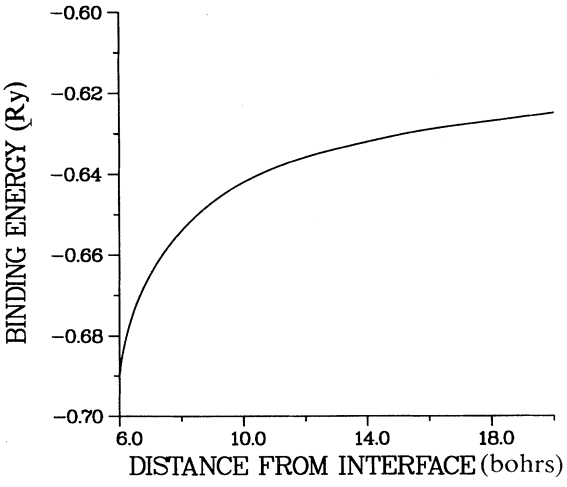

FIG. 6. Increase of the electronic binding energy as a function of ion nucleus-metal surface distance. (0.60 Ry=8.16 eV, 0.70 Ry=9.52 eV.)

The deeper potential well generated by the metal-electrolyte interference would also affect the binding energy of any excited state sustained by the bulk excess-electron complex. It is known that a chlorine anion in vacuum does not bind an excited bound state,[28] but the hydrated anion displays a broad absorption band centered near 1800 Å.[29] Since the metal-electrolyte potential well evolves into the isolated Landau potential with increasing distance from the interface, one would expect the modified potential well to feature an excited bound state for sufficiently large metal-anion separation. Alternatively, the deeper modified potential well might sustain a new excited state which would only be resolvable in the near interface region of the solvent. A possible method for calculating the excited-state binding energy would be to impose *s*-state symmetry on the successive trial wave functions, which would block convergence to the ground *p* state.

CONCLUSION

Our results for the ammoniated Cl^- ion problem show that the presence of a flat metal surface lowers the electronic binding energy by 1 eV if the ion nucleus is positioned $6.0a_0$ from the interface. The oxidation-reduction pair energy difference at this distance can then be determined by comparing the electronic binding energy before and after the polar molecules have reacted to the presence of the excess charge. In this case, the binding energy without the contribution from the oriented dipoles in 0.452 Ry; consequently the oxidation-reduction pair energy difference is 0.238 Ry or 3.2 eV. For the $10.0a_0$ case we have determined the complete binding energy to be 0.642 Ry so that the oxidation-reduction energy difference increases to 0.266 Ry or 3.6 eV. We therefore observe a shift in the oxidation-reduction pair energy difference of 0.4 eV as the complex approaches the metal surface by $4a_0$. The bulk value of the oxidation-reduction pair energy difference is obtained by setting the electron-electron image term to zero and subtracting the electron affinity from the complete binding energy of the isolated state. This yields an oxidation-reduction pair energy difference of 0.35 Ry or 4.8 eV. Thus the oxidation-reduction pair energy difference drops by 1.6 eV as the complex moves from the bulk to a position of $6.0a_0$ from a flat metal surface.

Since the binding energy of the Cl^- electron is 9.4 eV at a distance of $6.0a_0$ from the interface and typical met-

al work functions are in the range of 2–5 eV, our solvated anionic excess electron is prevented from entering the Fermi level of the metal by an energy barrier of at least several eV. Solvated electrons, however, have ionization energies of about 2 eV with typical conduction-band widths being in the range of 1–2 eV. Thus a solvated electronic state formed near a metal surface will not be stable if the excess electronic configuration energy is above the Fermi level of the metal. In this situation it becomes more energetically favorable for the excess electron to enter the lowest unoccupied state within the metal thereby removing the excess charge from the polar liquid. Since the medium is now neutral, the aligned polar molecules become disoriented and the induced image charge vanishes. A similar effect may occur with weakly bound solvated anionic excess electrons.

[1]J. Jortner, J. Chem. Phys. **30**, 839 (1959).
[2]J. Jortner, J. Chem. Phys. **27**, 823 (1957).
[3]D. A. Copeland, N. R. Kestner, and J. Jortner, J. Chem. Phys. **53**, 1189 (1970).
[4]B. C. Webster and I. C. Carmichael, J. Chem. Phys. **68**, 4086 (1978).
[5]P. Stampfli and K. H. Benneman, Phys. Rev. Lett. **58**, 2635 (1987).
[6]R. N. Barnett, U. Landman, C. L. Cleveland, and J. Jortner, Phys. Rev. Lett. **59**, 811 (1987).
[7]A. Wallqvist, D. Thirumalai, and B. J. Berne, J. Chem. Phys. **85**, 1583 (1986).
[8]E. Glueckauf, Trans. Faraday Soc. **60**, 1637 (1964).
[9]D. L. Beveridge and G. W. Schnuelle, J. Phys. Chem. **79**, 2562 (1975).
[10]M. H. Abraham and J. Liszi, J. Chem. Soc. Faraday Trans. I **74**, 1604 (1978).
[11]M. H. Abraham, J. Liszi, and L. Meszaros, J. Chem. Phys. **70**, 2491 (1979).
[12]R. Contreras and A. Aizman, Int. J. Quantum. Chem. **23**, 293 (1985).
[13]S. Ray, Chem. Phys. Lett. **11**, 573 (1971).
[14]S. Yamabe, S. Kato, H. Fujimoto, and K. Fukui, Theoret. Chim. Acta **30**, 327 (1973).
[15]J. B. Foresman and C. L. Brooks III, J. Chem. Phys. **87**, 5892 (1987).
[16]J. O. Noell and K. Morokuma, Chem. Phys. Lett. **36**, 465 (1975).
[17]P. S. Ganas, L. P. Gately, and T. Arakelian, Phys. Rev. A **30**, 2958 (1984).
[18]R. H. Stokes, J. Am. Chem. Soc. **86**, 979 (1964).
[19]D. Kosloff and R. Kosloff, J. Comput. Phys. **52**, 35 (1983).
[20]G. Dahlquist and Å Björck, *Numerical Methods* (Prentice Hall, Englewood Cliffs, NJ, 1974), Chap. 5.
[21]James H. Wilkinson, *The Algebraic Eigenvalue Problem* (Clarendon, Oxford, 1965), Chap. 9.
[22]Carl de Boor, *A Practical Guide To Splines* (Springer-Verlag, New York, 1978).
[23]A. K. Cline, *Fitpak– A Curve and Surface Fitting Package* (Pleasant Valley Software, Austin, TX, 1986).
[24]*CRC Handbook of Chemistry and Physics,* 69th ed., edited by Robert C. Weast (CRC, Boca Raton, FL, 1988), p. *E*-50.
[25]A. E. S. Green, D. L. Sellin, and A. S. Zachor, Phys. Rev. **184**, 1 (1969).
[26]P. Delahay, Acc. Chem. Res. **51**, 40 (1982).
[27]R. E. Ballard, J. Jones, E. Sutherland, and B. L. Chun, Chem. Phys. Lett. **97**, 419 (1983).
[28]Sir Harrie Massey, *Negative Ions* (Cambridge University Press, Cambridge, 1976), pp. 66 and 67.
[29]R. Platzman and J. Franck, Z. Phys. **138**, 411 (1954).